NASA/TM—2019—000000

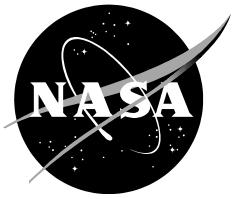

TESS Data Release Notes:
Sector 15, DR21

Michael M. Fausnaugh, Christopher J. Burke
Kavli Institute for Astrophysics and Space Science, Massachusetts Institute of Technology, Cambridge, Massachusetts

Douglas A. Caldwell
SETI Institute, Mountain View, California

Jon M. Jenkins
NASA Ames Research Center, Moffett Field, California

Jeffrey C. Smith, Joseph D. Twicken
SETI Institute, Mountain View, California

Roland Vanderspek
Kavli Institute for Astrophysics and Space Science, Massachusetts Institute of Technology, Cambridge, Massachusetts

John P. Doty
Noqsi Aerospace Ltd, Billerica, Massachusetts

Eric B. Ting
Ames Research Center, Moffett Field, California

Joel S. Villasenor
Kavli Institute for Astrophysics and Space Science, Massachusetts Institute of Technology, Cambridge, Massachusetts

October 03, 2019

NASA STI Program ... in Profile

Since its founding, NASA has been dedicated to the advancement of aeronautics and space science. The NASA scientific and technical information (STI) program plays a key part in helping NASA maintain this important role.
The NASA STI program operates under the auspices of the Agency Chief Information Officer. It collects, organizes, provides for archiving, and disseminates NASA's STI. The NASA STI program provides access to the NTRS Registered and its public interface, the NASA Technical Reports Server, thus providing one of the largest collections of aeronautical and space science STI in the world. Results are published in both non-NASA channels and by NASA in the NASA STI Report Series, which includes the following report types:

- TECHNICAL PUBLICATION. Reports of completed research or a major significant phase of research that present the results of NASA Programs and include extensive data or theoretical analysis. Includes compilations of significant scientific and technical data and information deemed to be of continuing reference value. NASA counterpart of peer-reviewed formal professional papers but has less stringent limitations on manuscript length and extent of graphic presentations.

- TECHNICAL MEMORANDUM.
  Scientific and technical findings that are preliminary or of specialized interest, e.g., quick release reports, working papers, and bibliographies that contain minimal annotation. Does not contain extensive analysis.

- CONTRACTOR REPORT. Scientific and technical findings by NASA-sponsored contractors and grantees.

- CONFERENCE PUBLICATION.
  Collected papers from scientific and technical conferences, symposia, seminars, or other meetings sponsored or co-sponsored by NASA.

- SPECIAL PUBLICATION.
  Scientific, technical, or historical information from NASA programs, projects, and missions, often concerned with subjects having substantial public interest.

- TECHNICAL TRANSLATION.
  English-language translations of foreign scientific and technical material pertinent to NASA's mission.

Specialized services also include organizing and publishing research results, distributing specialized research announcements and feeds, providing information desk and personal search support, and enabling data exchange services.

For more information about the NASA STI program, see the following:

- Access the NASA STI program home page at http://www.sti.nasa.gov

- E-mail your question to help@sti.nasa.gov

- Phone the NASA STI Information Desk at 757-864-9658

- Write to:
  NASA STI Information Desk
  Mail Stop 148
  NASA Langley Research Center
  Hampton, VA 23681-2199

NASA/TM—2019—000000

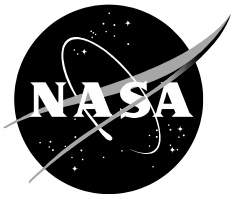

TESS Data Release Notes:
Sector 15, DR21

Michael M. Fausnaugh, Christopher J. Burke
Kavli Institute for Astrophysics and Space Science, Massachusetts Institute of Technology, Cambridge, Massachusetts

Douglas A. Caldwell
SETI Institute, Mountain View, California

Jon M. Jenkins
NASA Ames Research Center, Moffett Field, California

Jeffrey C. Smith, Joseph D. Twicken
SETI Institute, Mountain View, California

Roland Vanderspek
Kavli Institute for Astrophysics and Space Science, Massachusetts Institute of Technology, Cambridge, Massachusetts

John P. Doty
Noqsi Aerospace Ltd, Billerica, Massachusetts

Eric B. Ting
Ames Research Center, Moffett Field, California

Joel S. Villasenor
Kavli Institute for Astrophysics and Space Science, Massachusetts Institute of Technology, Cambridge, Massachusetts

October 03, 2019

Acknowledgements

These Data Release Notes provide information on the processing and export of data from the Transiting Exoplanet Survey Satellite (TESS). The data products included in this data release are full frame images (FFIs), target pixel files, light curve files, collateral pixel files, cotrending basis vectors (CBVs), and Data Validation (DV) reports, time series, and associated xml files.

These data products were generated by the TESS Science Processing Operations Center (SPOC, Jenkins et al., 2016) at NASA Ames Research Center from data collected by the TESS instrument, which is managed by the TESS Payload Operations Center (POC) at Massachusetts Institute of Technology (MIT). The format and content of these data products are documented in the Science Data Products Description Document (SDPDD)[1]. The SPOC science algorithms are based heavily on those of the Kepler Mission science pipeline, and are described in the Kepler Data Processing Handbook (Jenkins, 2017).[2] The Data Validation algorithms are documented in Twicken et al. (2018) and Li et al. (2019). The TESS Instrument Handbook (Vanderspek et al., 2018) contains more information about the TESS instrument design, detector layout, data properties, and mission operations.

The TESS Mission is funded by NASA's Science Mission Directorate.

This report is available in electronic form at
https://archive.stsci.edu/tess/

[1] https://archive.stsci.edu/missions/tess/doc/EXP-TESS-ARC-ICD-TM-0014.pdf
[2] https://archive.stsci.edu/kepler/manuals/KSCI-19081-002-KDPH.pdf

1 Observations

TESS Sector 15 observations include physical orbits 37 and 38 of the spacecraft around the Earth. Data collection was paused for 1.08 days during perigee passage while downloading data. In total, there are 24.97 days of science data collected in Sector 15.

Table 1: Sector 15 Observation times

	UTC	TJD[a]	Cadence #
Orbit 37 start	2019-08-15 20:35:28	1711.35947	348411
Orbit 37 end	2019-08-28 08:31:28	1723.85669	357409
Orbit 38 start	2019-08-29 10:25:28	1724.93585	358186
Orbit 38 end	2019-09-10 21:47:27	1737.40946	367167

[a] TJD = TESS JD = JD - 2,457,000.0

The spacecraft was pointing at RA (J2000): 280.3985°; Dec (J2000): 64.0671°; Roll: 55.4277°. Two-minute cadence data were collected for 19,999 targets, and full frame images were collected every 30 minutes. See the TESS project Sector 15 observation page[3] for the coordinates of the spacecraft pointing and center field-of-view of each camera, as well as the detailed target list. Fields-of-view for each camera and the Guest Investigator two-minute target list can be found at the TESS Guest Investigator Office observations status page[4].

1.1 Notes on Individual Targets

Three very bright stars (Tmag $\lesssim$ 1.8) with large pixel stamps were not processed in the photometric pipeline. Target pixel files with raw data are provided, but no light curves were produced. The affected TIC IDs are 229540730, 232853959, and 150387644.

Fourteen target stars (159190000, 159190005, 165602000, 165602023, 341873045, 389917321, 441804565, 471011825, 471011933, 1102642384 471012067, 1551711135, 1972296808, 289622291) are blended with comparably bright stars—the contaminating flux for these objects is very large, and the resulting photometry for such targets is expected to be unreliable.

Two stars (186136107 and 13415581) are close enough to bleed trails from brighter stars that the photometry is likely unreliable.

1.2 Spacecraft Pointing and Momentum dumps

As in Sector 14, the pointing in Sector 15 was set at +85 degrees in ecliptic latitude, so that Camera 2 and Camera 3 straddle the ecliptic pole. Camera 1 still suffers from strong scattered light signals (see §1.3), and so guiding was disabled in Camera 1 for both orbits 37 and 38. Camera 4 alone was used for guiding during this sector.

The reaction wheel speeds were reset with momentum dumps every 4.25 days. Figure 1 summarizes the pointing performance over the course of the sector based on Fine Pointing telemetry.

[3] https://tess.mit.edu/observations/sector-15

[4] https://heasarc.gsfc.nasa.gov/docs/tess/status.html

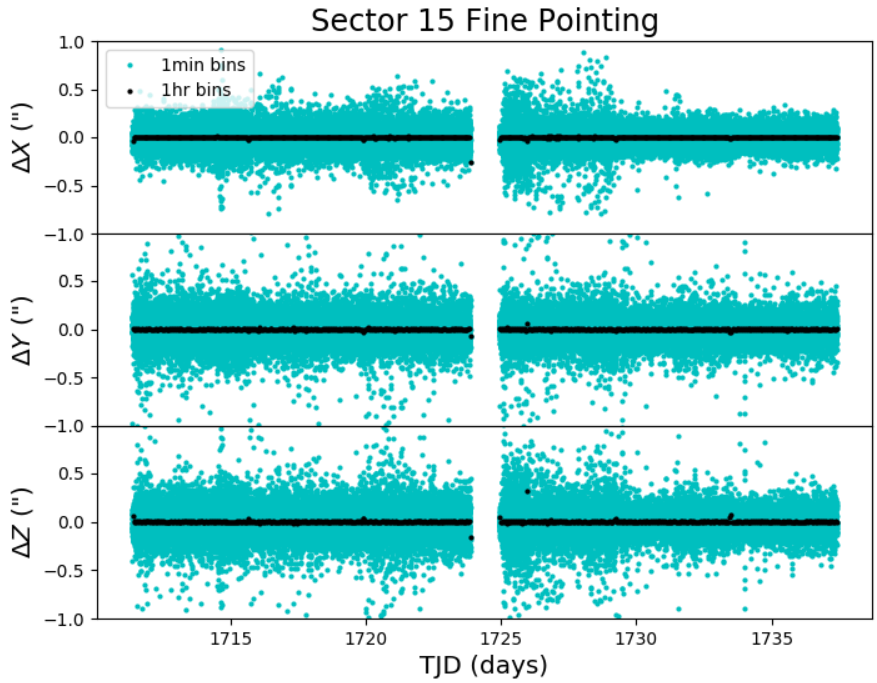

Figure 1: Guiding corrections based on spacecraft fine pointing telemetry. The delta-quaternions from each camera have been converted to spacecraft frame, binned to 1 minute and 1 hour, and averaged across cameras. Long-term trends (such as those caused by differential velocity aberration) have also been removed. The ΔX/ΔY directions represent offsets along the the detectors' rows/columns, while the ΔZ direction represents spacecraft roll.

Finally, a single upset event in the star trackers caused the spacecraft to fall out of fine pointing in orbit 38. The issue lasts for 5 minutes at TJD 1725.93651 (cadences 358907, 358908, and 358909). The same issue was observed for a longer period of time in Sector 13 (see DRN 18[5]).

1.3 Scattered Light

Figure 2 shows the median value of the background estimate for all targets on a given CCD as a function of time. Figure 3 shows the angle between each camera's boresight and the Earth or Moon—this figure can be used to identify periods affected by scattered light and the relative contributions of the Earth and Moon to the image backgrounds.

In Sector 15, the Earth is above the sunshade for almost the entire sector, similar to Sector 14. The 24 hour rotation period of the Earth and several harmonics thereof are visible as oscillations in the background for most of both orbits. Finally, the Earth passes close to Camera 1 towards the last quarter of each orbit and saturates the detectors—these times were excluded with CCD-specific "Scattered Light" flags.

[5] https://archive.stsci.edu/missions/tess/doc/tess_drn/tess_sector_13_drn18_v02.pdf

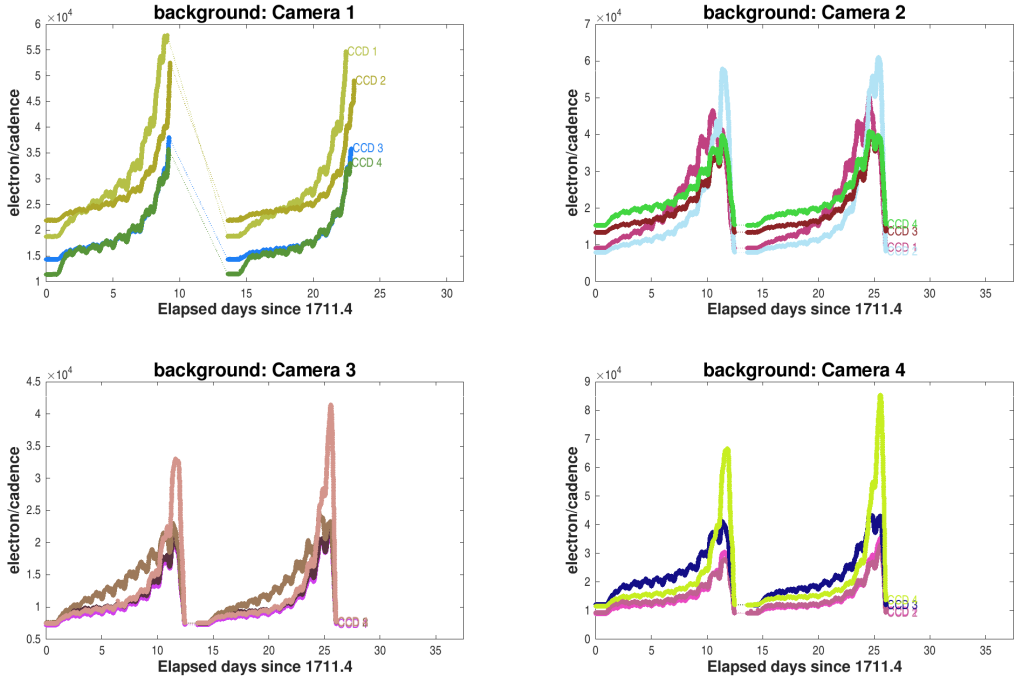

Figure 2: Median background flux across all targets on a given CCD in each camera. The changes are caused by variations in the orientation and distance of the Earth and Moon.

2 Data Anomaly Flags

See the SDPDD (§9) for a list of data quality flags and the associated binary values used for TESS data, and the TESS Instrument Handbook for a more detailed description of each flag.

The following flags were not used in Sector 15: bits 1, 2, 7, 9, and 11 (Attitude Tweak, Safe Mode, Cosmic Ray in Aperture, Discontinuity, Cosmic Ray in Collateral Pixel).

Cadences marked with bits 3, 4, 6, and 12 (Coarse Point, Earth Point, Reaction Wheel Desaturation Event, and Straylight) were marked based on spacecraft telemetry.

Cadences marked with bit 5 and 10 (Argabrightening Events and Impulsive Outlier) were identified by the SPOC pipeline. Bit 5 marks a sudden change in the background measurements. In practice, bit 5 flags are caused by rapidly changing glints and unstable pointing at times near momentum dumps. Bit 10 marks an outlier identified by PDC and omitted from the cotrending procedure.

Cadences marked with bit 8 (Manual Exclude) are ignored by PDC, TPS, and DV for cotrending and transit searches. In Sector 15, these cadences were identified using spacecraft telemetry from the fine pointing system. All cadences with pointing excursions >21 arcseconds (∼1 pixel) were flagged for manual exclude. See Figure 4 for an assessment of the performance of the cotrending based on the final set of manual excludes.

In Sector 15, bit 13 (value 4096, "Scattered Light") was set based on the observed background measurements for targets on each CCD, in order to mask cadences that would neg-

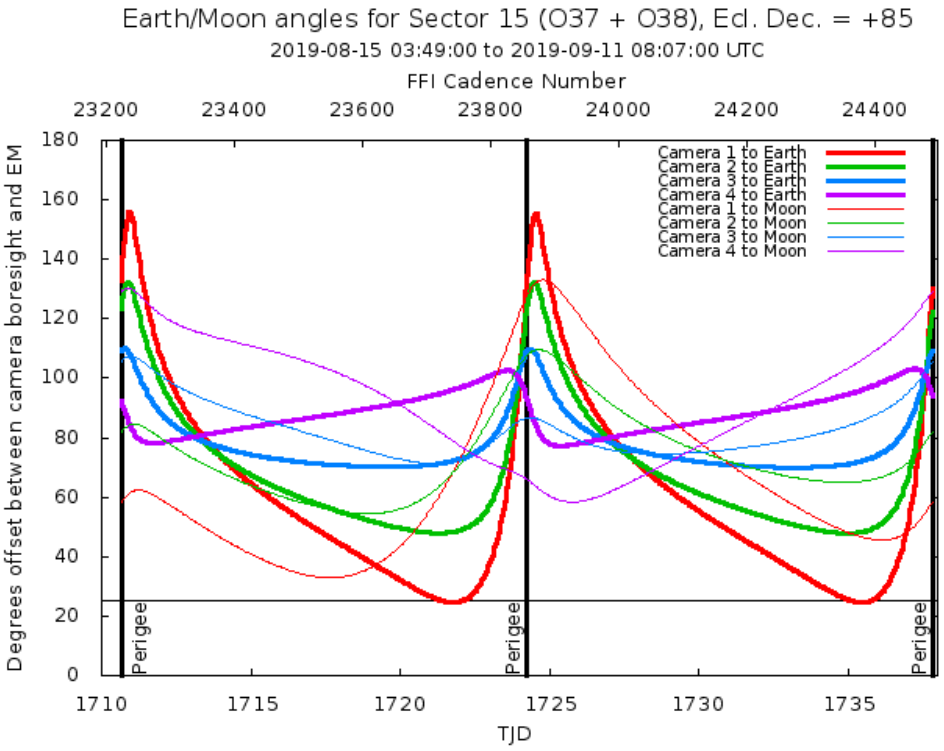

Figure 3: Angle between the four camera boresights and the Earth/Moon as a function of time. When the Earth is within $\sim 25°$ of a camera's boresight, transiting planet searches may be compromised by high levels of scattered light. At larger angles, up to $\sim 35°$, scattered light patterns and complicated structures may be visible. At yet larger angles, low level patchy features may be visible. Scattered light from the Moon is generally only noticeable below $\sim 35°$. This figure can be used to identify periods affected by scattered light and the relative contributions of the Earth and Moon to the background. However, the background intensity and locations of scattered light features depend on additional factors, such as the Earth/Moon azimuth and distance from the spacecraft.

atively affect the systematic error removal in PDC and the planet search in TPS. This flag was introduced in Sector 14.

FFIs were only marked with bits 3, 6 and 12 (Course Point, Reaction Wheel Desaturation Events and Straylight). Only one FFI is affected by each momentum dump.

3 Anomalous Effects

3.1 Smear Correction Issues

The following columns were impacted by bright stars in the science frame, and/or upper buffer rows, which bleed into the upper serial register resulting in an overestimated smear correction.

- Camera 1, CCD 2, Column 783, Star Epsilon Cygni

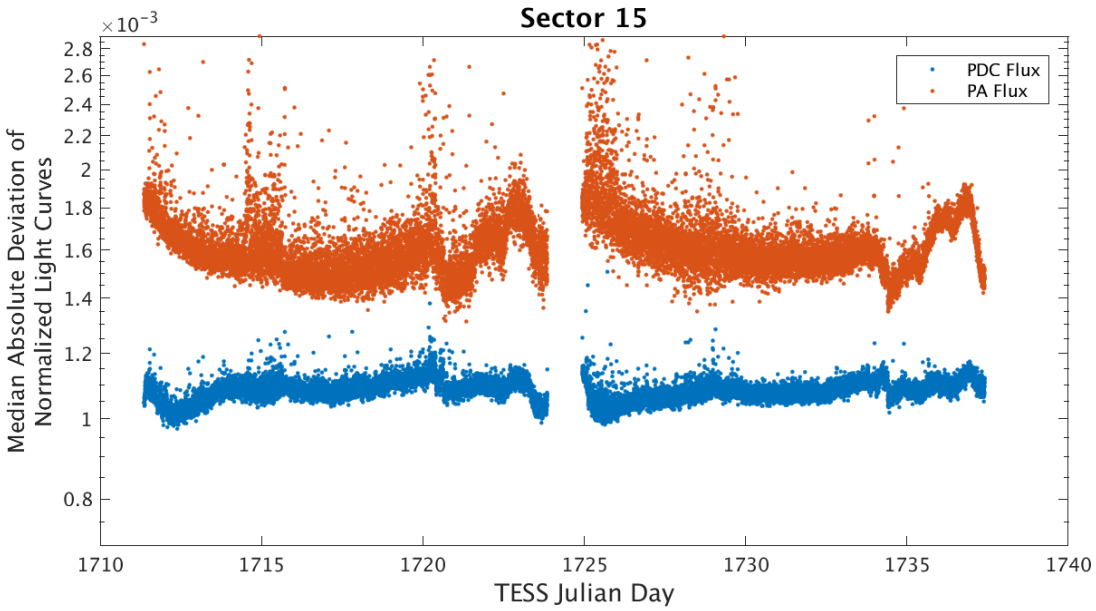

Figure 4: Median absolute deviation (MAD) for the 2-minute cadence data from Sector 15, showing the performance of the cotrending after identifying Manual Exclude data quality flags. The MAD is calculated in each cadence across stars with flux variations less than 1% for both the PA (red) and PDC (blue) light curves, where each light curve is normalized by its median flux value. The scatter in the PA light curves is much higher than that for the PDC light curves, and the outliers in the PA light curves are largely absent from the PDC light curves due to the use of the anomaly flags.

- Camera 3, CCD 4, Column 683, Star 18 Draconis
- Camera 4, CCD 1, Column 723, Star 84 Ursae Majoris
- Camera 4, CCD 3, Column 943, Star HD 107155
- Camera 4, CCD 3, Column 1638, Star HD 111270
- Camera 4, CCD 4, Column 1293, Star 83 Ursae Majoris

3.2 Fireflies and Fireworks

Table 2 lists all firefly and fireworks events for Sector 15. These phenomena are small, spatially extended, comet-like features in the images—created by sunlit particles in the camera FOV—that may appear one or two at a time (fireflies) or in large groups (fireworks). See the TESS Instrument Handbook for a more complete description.

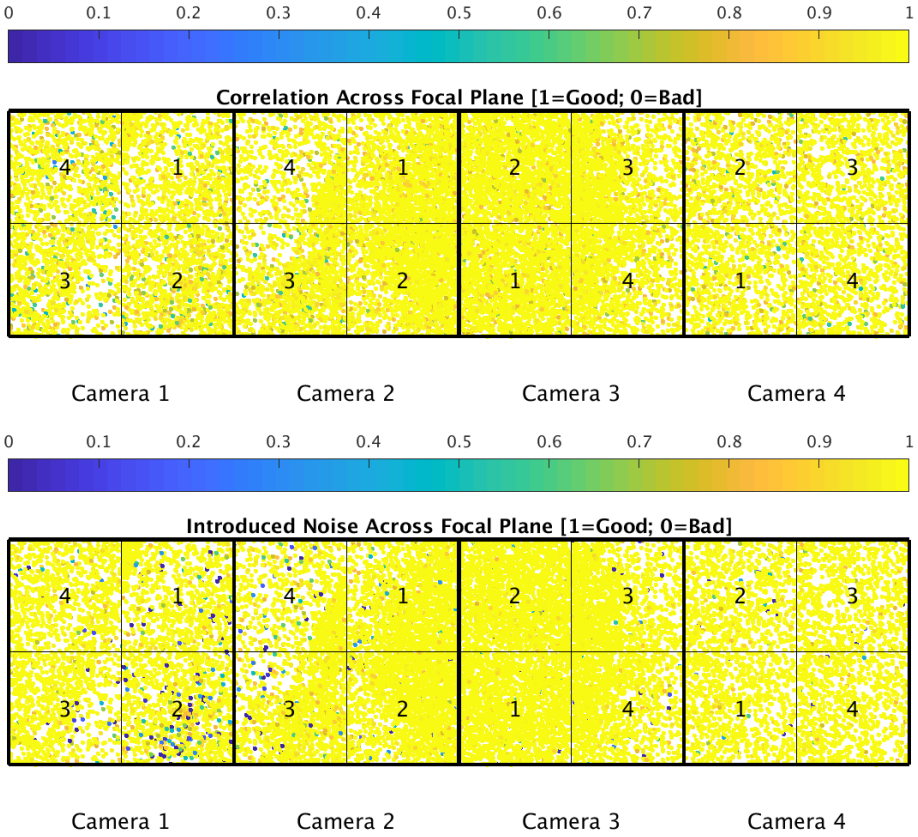

Figure 5: PDC residual correlation goodness metric (top panel) and PDC introduced noise goodness metric (bottom panel). The metric values are shown on a focal plane map indicating the camera and CCD location of each target. The correlation goodness metric is calibrated such that a value greater than 0.8 means there is less than 10% mean absolute correlation between the target under study and all other targets on the CCD. The introduced noise metric is calibrated such that a value greater than 0.8 means the power in broad-band introduced noise is below the level of uncertainties in the flux values.

4 Pipeline Performance and Results

4.1 Light Curves and Photometric Precision

Figure 5 gives the PDC goodness metrics for residual correlation and introduced noise on a scale between 0 (bad) and 1 (good). The performance of PDC is very good and generally uniform over most of the field of view. Figure 6 shows the achieved Combined Differential Photometric Precision (CDPP) at 1-hour timescales for all targets.

4.2 Transit Search and Data Validation

In Sector 15, the light curves of 19999 targets were subjected to the transit search in TPS. Of these, Threshold Crossing Events (TCEs) at the 7.1 σ level were generated for 858 targets.

As in Sector 14, we employed an iterative method when conducting the Sector 15 transit

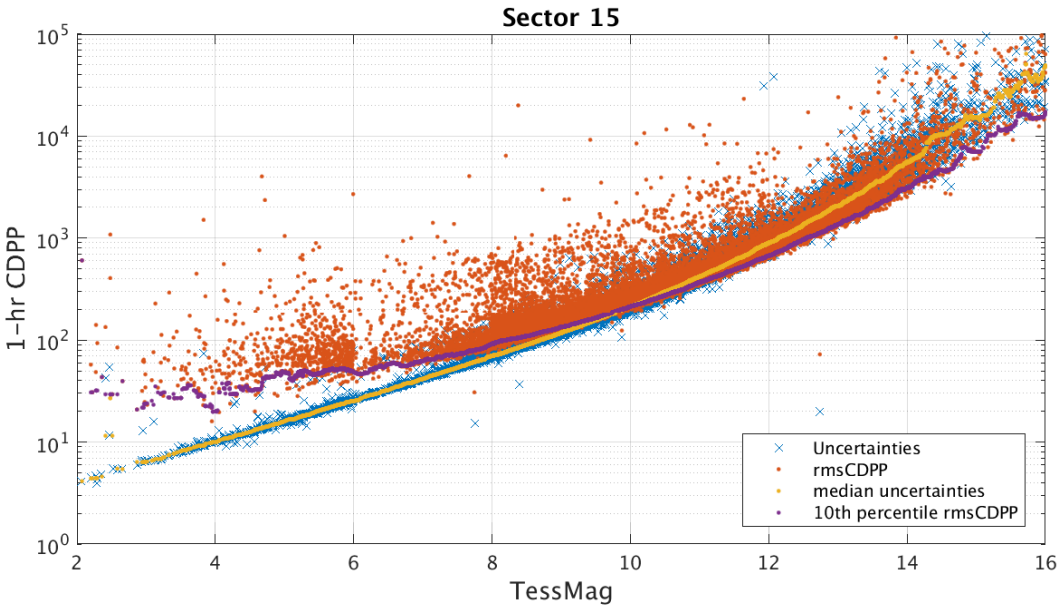

Figure 6: 1-hour CDPP. The red points are the RMS CDPP measurements for the 19999 light curves from Sector 15 plotted as a function of TESS magnitude. The blue x's are the uncertainties, scaled to 1-hour timescale. The purple curve is a moving 10th percentile of the RMS CDPP measurements, and the gold curve is a moving median of the 1-hr uncertainties.

Table 2: Sector Fireflies and Fireworks

FFI Start	FFI End	Cameras	Description
2019234065928	2019234072928	2, 3, 4	Fireflies
2019234155928	2019234162928	2, 4	Fireflies
2019241185928	2019241192928	4	Firefly
2019242222928	2019242225928	3	Firefly
2019248202928	2019248205928	3, 4	Firefly

search. The top panel of Figure 7 shows the number of TCEs at a given cadence that exhibit a transit signal from an initial run of TPS. The $3\,\sigma$ peaks were used to define deemphasis weights for a second run of TPS, the results of which are shown in the bottom panel of Figure 7. The final set of TCEs and the results reported here are based on the second run of TPS. The values of the adopted deemphasis weights are provided in the DV timeseries data products for targets with TCEs.

The top panel of Figure 8 shows the distribution of orbital periods for the final set of TCEs found in Sector 15. The vertical histogram in the right panel of Figure 8 shows the distribution of transit depths derived from limb-darkened transiting planet model fits for TCEs. The model transit depths range down to the order of 100 ppm, but the bulk of the transit depths are considerably larger.

A search for additional TCEs in potential multiple planet systems was conducted in DV through calls to TPS. A total of 1296 TCEs were ultimately identified in the SPOC pipeline

on 858 unique target stars. Table 3 provides a breakdown of the number of TCEs by target. Note that targets with large numbers of TCEs are likely to include false positives.

Finally, the difference images and associated centroid offset figures in the DV reports have limits applied to the number and magnitude of displayed stars, in order to make sure that the images are not completely covered by labels in crowded regions of the sky.

Table 3: Sector 15 TCE Numbers

Number of TCEs	Number of Targets	Total TCEs
1	520	520
2	264	528
3	52	156
4	19	76
5	2	10
6	1	6
–	858	1296

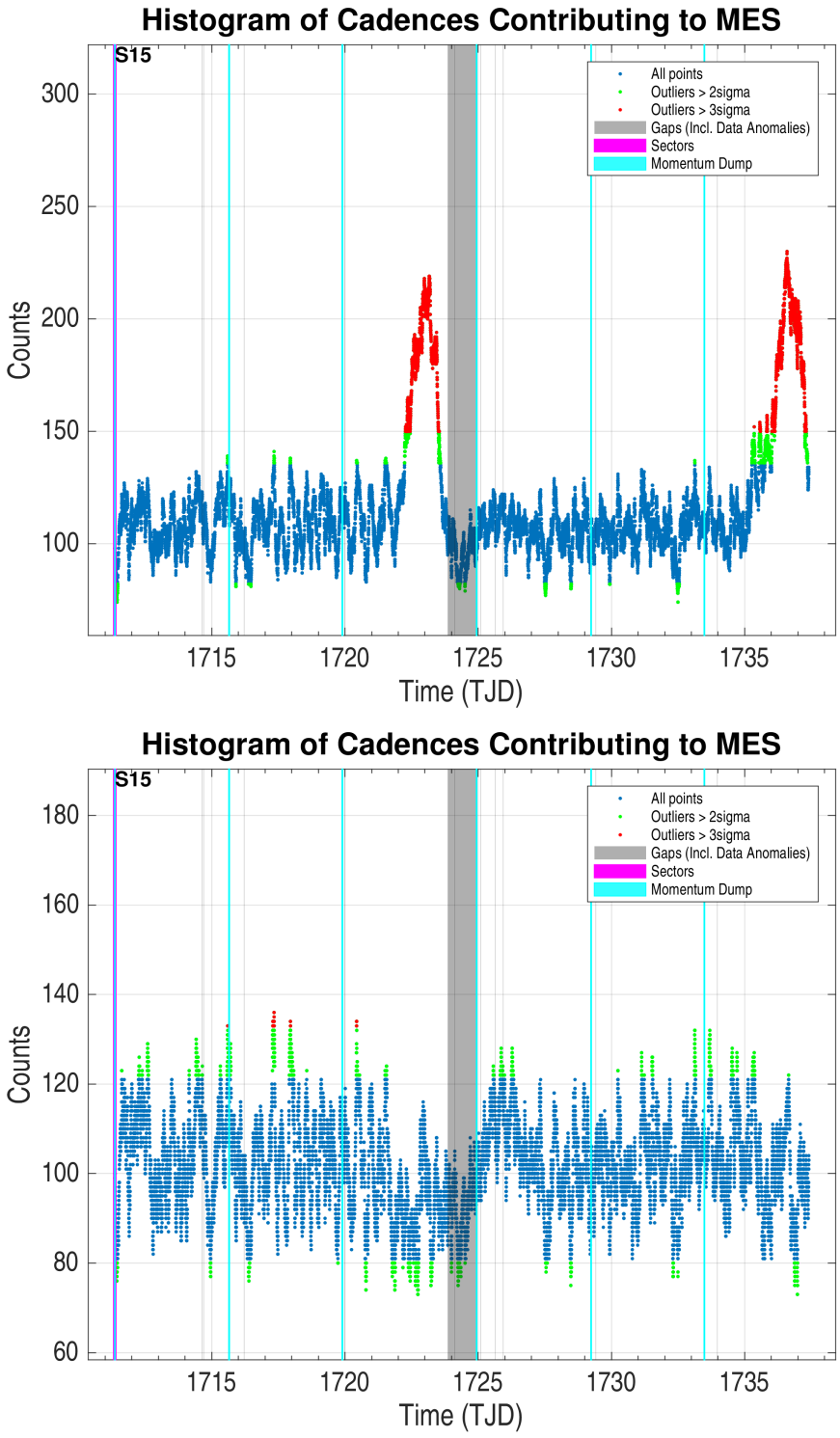

Figure 7: Top panel: Number of TCEs at a given cadence exhibiting a transit signal, based on an initial run of TPS. Any isolated peaks are caused by single events that result in spurious TCEs. These peaks were used to define deemphasis weights that suppress the contribution of problematic epochs to the transit detection statistics in a second iteration of TPS. Bottom panel: Results from the second run of TPS.

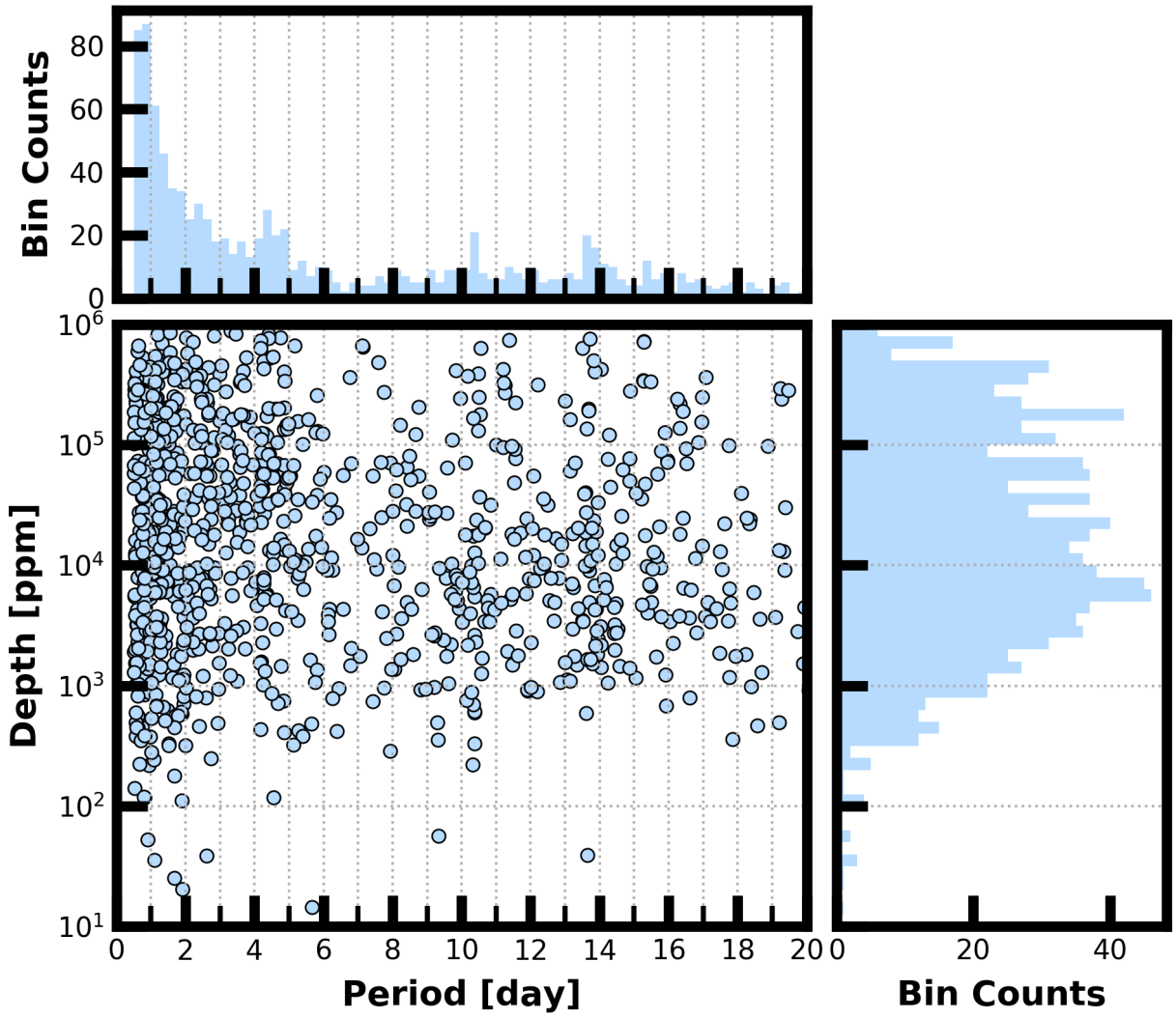

Figure 8: Lower Left Panel: Transit depth as a function of orbital period for the 1296 TCEs identified for the Sector 15 search. For enhanced visibility of long period detections, TCEs with orbital period <0.5 days are not shown. Reported depth comes from the DV limb darkened transit fit depth when available, and the DV trapezoid model fit depth when not available. Top Panel: Orbital period distribution of the TCEs shown in the lower left panel. Right Panel: Transit depth distribution for the TCEs shown in the lower left panel.

References

Jenkins, J. M. 2017, Kepler Data Processing Handbook: Overview of the Science Operations Center, Tech. rep., NASA Ames Research Center

Jenkins, J. M., Twicken, J. D., McCauliff, S., et al. 2016, in Proc. SPIE, Vol. 9913, Software and Cyberinfrastructure for Astronomy IV, 99133E

Li, J., Tenenbaum, P., Twicken, J. D., et al. 2019, *PASP*, 131, 024506, doi: 10.1088/1538-3873/aaf44d

Twicken, J. D., Catanzarite, J. H., Clarke, B. D., et al. 2018, *PASP*, 130, 064502, doi: 10.1088/1538-3873/aab694

Vanderspek, R., Doty, J., Fausnaugh, M., et al. 2018, TESS Instrument Handbook, Tech. rep., Kavli Institute for Astrophysics and Space Science, Massachusetts Institute of Technology

Acronyms and Abbreviation List

BTJD Barycentric-corrected TESS Julian Date

CAL Calibration Pipeline Module

CBV Cotrending Basis Vector

CCD Charge Coupled Device

CDPP Combined Differential Photometric Precision

COA Compute Optimal Aperture Pipeline Module

CSCI Computer Software Configuration Item

CTE Charge Transfer Efficiency

Dec Declination

DR Data Release

DV Data Validation Pipeline Module

DVA Differential Velocity Aberration

FFI Full Frame Image

FIN FFI Index Number

FITS Flexible Image Transport System

FOV Field of View

FPG Focal Plane Geometry model

KDPH Kepler Data Processing Handbook

KIH Kepler Instrument Handbook

KOI Kepler Object of Interest

MAD Median Absolute Deviation

MAP Maximum A Posteriori

MAST Mikulski Archive for Space Telescopes

MES Multiple Event Statistic

NAS NASA Advanced Supercomputing Division

PA Photometric Analysis Pipeline Module

PDC Pre-Search Data Conditioning Pipeline Module

PDC-MAP Pre-Search Data Conditioning Maximum A Posteriori algorithm

PDC-msMAP Pre-Search Data Conditioning Multiscale Maximum A Posteriori algorithm

PDF Portable Document Format

POC Payload Operations Center

POU Propagation of Uncertainties

ppm Parts-per-million

PRF Pixel Response Function

RA Right Ascension

RMS Root Mean Square

SAP Simple Aperture Photometry

SDPDD Science Data Product Description Document

SNR Signal-to-Noise Ratio

SPOC Science Processing Operations Center

SVD Singular Value Decomposition

TCE Threshold Crossing Event

TESS Transiting Exoplanet Survey Satellite

TIC TESS Input Catalog

TIH TESS Instrument Handbook

TJD TESS Julian Date

TOI TESS Object of Interest

TPS Transiting Planet Search Pipeline Module

UTC Coordinated Universal Time

XML Extensible Markup Language